complex, from which the benzoate and chloride complexes were prepared by the above metathesis procedure.

Mn(TMP)Bzo. Mn(TMP)Cl was the generous gift of Dr. Scott Raybuck and was used in the above metathesis procedure to prepare the benzoate complex.

Electrochemical Instrumentation. Cyclic voltammetry was performed with a potentiostat and waveform generator of local construction. Rotated-disk voltammetry was performed with the same potentiostatic hardware and a Pine Instruments Model ASR-2 variable-speed analytical rotator. Chronoamperometry and controlled-potential electrolysis experiments were performed with a PAR 173 potentiostat and PAR 176 current-to-voltage converter. Potential steps were generated and current–time data recorded with the aid of an IBM-PC computer with a Tecmar Labmaster 12-bit analog-to-digital converter. In chronoamperometry experiments, background currents were recorded on blank solutions and subtracted digitally.

Electrochemical Experiments. All experiments were performed in dichloromethane–0.2 M n-Bu_4NClO_4. Glassy-carbon-disk working electrodes (Atomergic, grade V-10, 0.057 cm^2) were pressure-fitted into Teflon, polished with 1-μm diamond paste (Buehler) on a manila surface and rinsed with copious quantities of water and dichloromethane. Potentials are reported vs. the NaCl saturated calomel electrode (NaSCE). Solutions were purged with argon and oxygenated with pure oxygen.

Cyclic voltammetry and rotated-disk voltammetry were performed in a conventional two-component cell with the working electrode and platinum-wire counter electrode in the same compartment. Chronoamperometry was performed in a similar cell, except that a Luggin capillary connected the cell compartments, to diminish the effects of uncompensated solution resistance. Controlled-potential electrolysis experiments were performed with a glassy-carbon crucible (Atomergic, grade V-25) as both working electrode and reaction vessel.

Acknowledgment. Helpful discussions with Prof. J. P. Collman and J. Fitzgerald of Stanford University and Dr. Scott Raybuck of the Massachusetts Institute of Technology are gratefully acknowledged. This work was supported in part by a grant from the National Science Foundation. S.E.C. acknowledges support from the 1986 Edward G. Weston Fellowship of The Electrochemical Society.

Contribution from the Departments of Chemistry, University of Denver, Denver, Colorado 80208, and University of Colorado at Denver, Denver, Colorado 80202

Metal–Nitroxyl Interactions. 52. EPR Spectra of Nitroxyl Radicals Coordinated to Manganese(III) Tetraphenylporphyrin via the Nitroxyl Oxygen

Kundalika M. More, Gareth R. Eaton,* and Sandra S. Eaton*

Received February 24, 1987

EPR spectra of six nitroxyl radicals coordinated to manganese(III) tetraphenylporphyrin via the nitroxyl oxygen were examined in frozen toluene solution. Antiferromagnetic coupling between the $S = 2$ Mn(III) and the $S = {}^1/_2$ nitroxyl states resulted in an $S = {}^3/_2$ ground state. The observed effective g values of 4.0 and 2.0 are characteristic of zero-field splitting greater than the EPR quantum. Resolved nuclear hyperfine splitting was observed on the $g = 4$ signal. The antiferromagnetic interaction was sufficiently strong that the $S = {}^5/_2$ excited state was not detected at 100 K.

Introduction

Electron–electron spin–spin interaction between nitroxyl radicals and paramagnetic transition metals has been observed in two classes of compounds.[1] (1) The nitroxyl is part of a ligand that is bound to the metal by an atom other than the nitroxyl oxygen. (2) The nitroxyl oxygen is coordinated to the metal. For complexes of the first type, a range of magnitudes of spin–spin interaction has been analyzed by EPR.[1] For the second type of complex, relatively little EPR data have been obtained for the following reasons. Many of the studies of coordination of nitroxyl radicals to transition metals have used metals with $S = {}^1/_2$, particularly Cu(II). Spin–spin interaction between two $S = {}^1/_2$ centers results in a singlet (which does not give an EPR spectrum) and a triplet. When the nitroxyl oxygen is bound to the $S = {}^1/_2$ metal the M–O distance is about 2.0 to 2.5 Å.[2] As a result of the short interspin distance there is large dipolar interaction that can make detection of the triplet EPR signal difficult. In addition, in many of the cases that have been examined the spin–spin interaction is strongly antiferromagnetic and the population of the triplet is small. As a result no EPR spectra have been reported for complexes in which a nitroxyl oxygen is bound to a metal with $S = {}^1/_2$ and the coupling is antiferromagnetic. Triplet EPR spectra have been obtained for a complex with a nitroxyl oxygen bound to Cu(II) in which the coupling was ferromagnetic.[3] If the metal has $S > {}^1/_2$, spin coupling to one or more bound nitroxyl radicals can produce species with an odd number of unpaired electrons. EPR spectra should then be readily detectable for the lowest Kramer's doublets in these systems. Room-temperature EPR spectra in magnetically concentrated solids were recently reported for the $S = {}^3/_2$, ${}^5/_2$, and ${}^7/_2$ spin states that result from antiferromagnetic coupling between Mn(II) and two nitroxyl radicals.[4] In this paper we report that an $S = {}^3/_2$ spin state results when nitroxyl radicals I–VI are coordinated to Mn(III) tetraphenylporphyrin ($S = 2$) in dilute solution.

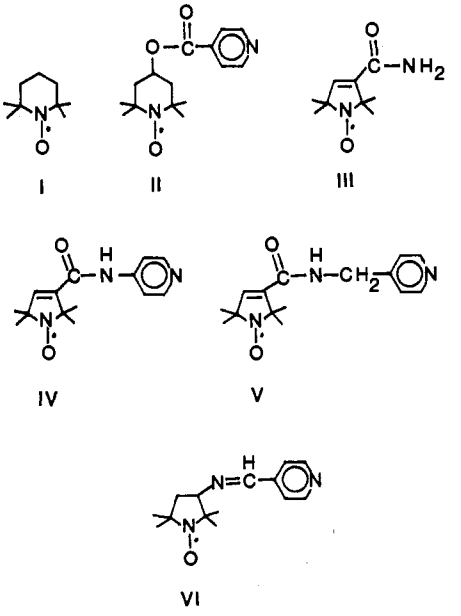

* To whom correspondence should be addressed: G.R.E., University of Denver; S.S.E., University of Colorado at Denver.

(1) Eaton, S. S.; Eaton, G. R. *Coord. Chem. Rev.*, in press.
(2) Felthouse, T. R.; Dong, T.-Y.; Hendrickson, D. N.; Shieh, H.-Y.; Thompson, M. R. *J. Am. Chem. Soc.* **1986**, *108*, 8201.
(3) Bencini, A.; Benelli, C.; Gatteschi, D.; Zanchini, C. *J. Am. Chem. Soc.* **1984**, *106*, 5813.
(4) Benelli, C.; Gatteschi, D.; Zanchini, C.; Doedens, R. J.; Dickman, M. H.; Porter, L. C. *Inorg. Chem.* **1986**, *25*, 3453.

0020-1669/87/1326-2618$01.50/0

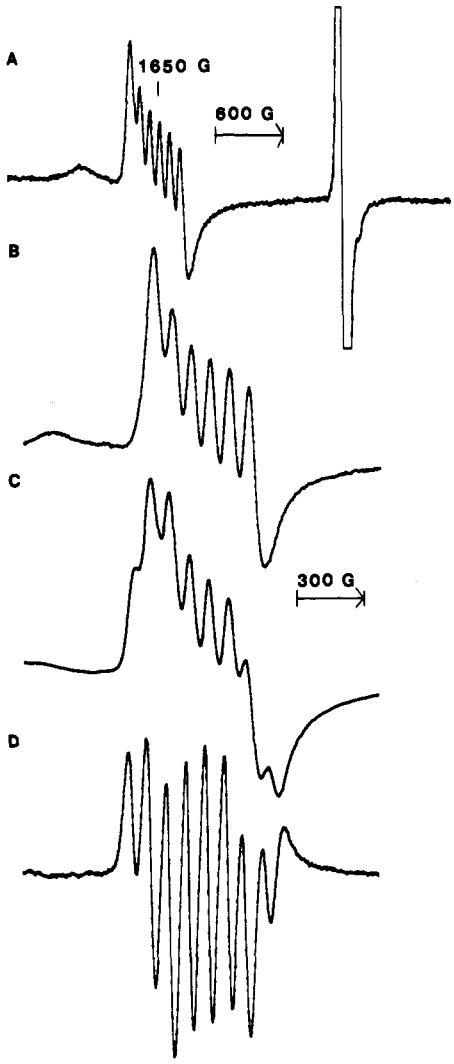

Figure 1. X-Band (9.102-GHz) EPR spectra in frozen toluene solution at 100 K: (A) 4000-G scan of a sample prepared with 2.0 mM Mn(TPP)ClO_4 and 2.0 mM nitroxyl I obtained with 10-G modulation amplitude and 50-mW microwave power; (B) 2000-G scan of the same sample used in part A; (C) 2000-G scan of a sample prepared with 5.0 mM Mn(TPP)ClO_4 and 3.0 mM nitroxyl IV obtained with 10-G modulation amplitude and 50-mW microwave power; (D) second derivative of the spectrum shown in part C.

Experimental Section

Manganese(III) tetraphenylporphyrin (Mn(TPP)) perchlorate,[5] II,[6] IV,[6] V,[7] and VI[8] were prepared by literature methods.

EPR spectra were obtained on a Varian E9 interfaced to an IBM CS9000 laboratory computer. Modulation amplitudes (100 kHz) were less than one-fifth of line widths and microwave powers were below the values that caused saturation of the signals. Second-derivative EPR spectra were obtained by simultaneously modulating at 1 kHz and 100 kHz.

Quantitation of the first-derivative EPR signals was done by comparison of double integrals of the spectra with double integrals of spectra of nitroxyl radicals at known concentration. Throughout the text integral is used to mean the second integral of the first-derivative EPR spectra.

Results and Discussion

The zero-field splitting (ZFS) for Mn(TPP)$ClO_4 \cdot 2H_2O$ is −2.3 cm^{-1}.[9] The EPR spectrum of Mn(TPP)ClO_4 in frozen toluene solution showed only a small broad signal with a peak at about $g = 7.8$. This indicated that most of the transitions for the $S = 2$ center were not observable at X-band, as expected for a system with an even number of unpaired electrons and ZFS greater than the EPR quantum (0.3 cm^{-1} at X-band). The ZFS for Mn(TPP)Cl, −1.8 to −1.9 cm^{-1},[9,10] and Mn(TPP)Cl(py), −3.0 cm^{-1},[10] also are greater than the EPR quantum at X-band.

When nitroxyl radical I was added to a toluene solution of Mn(TPP)ClO_4, the fluid-solution EPR spectrum was a typical three-line nitroxyl signal. The integrated intensity of the signal accounted for all of the nitroxyl in the sample. When the sample was frozen, the integrated intensity of the nitroxyl signal was less than that expected for 100% of the spins, which indicated that some of the nitroxyl was interacting with the Mn(TPP)ClO_4. A 4000-G scan of the spectrum is shown in Figure 1A. The assignments of the lines are as follows: broad peak at 830 G, Mn(TPP)ClO_4; six-line signal at $g = 4$, Mn(TPP)·I; off-scale signal at $g = 2$, I; and shoulder on the high-field side of the off-scale nitroxyl signal, Mn(TPP)·I. When excess pyridine was added to the solution, the signals for Mn(TPP)·I disappeared and the integrated intensity of the nitroxyl $g = 2$ signal accounted for all of the nitroxyl in the sample. Since the intensity of the nitroxyl signal was restored by pyridine displacement of the bound nitroxyl and since all of the nitroxyl intensity was observed in fluid solution, it is clear that the new signals in the frozen-solution EPR spectra were due to coordination of the nitroxyl and not to a redox reaction between the Mn(III) and nitroxyl.

Spin–spin interaction between $S = 2$ and $S = {}^1/_2$ gives $S = {}^3/_2$ and ${}^5/_2$ states. The manganese contribution to the ZFS in the coupled system is ${}^7/_5$ of the ZFS for the Mn(III) in the absence of interaction for the $S = {}^3/_2$ state and ${}^3/_5$ of the noninteracting value for the $S = {}^5/_2$ state.[11,12] Since the values of ZFS for Mn(TPP)ClO_4, Mn(TPP)Cl, and Mn(TPP)Cl(py) are greater than the EPR quantum at X-band, it seems plausible that the ZFS for Mn(TPP)·I would also be greater than the EPR quantum.

When the ZFS is greater than the EPR quantum, axially symmetric $S = {}^3/_2$ systems have characteristic spectra with $g_\parallel = 2$ and $g_\perp = 4$ and $S = {}^5/_2$ systems have $g_\parallel = 2$ and $g_\perp = 6$ due to observation of transitions within the $m_s = \pm{}^1/_2$ Kramer's doublet.[13] Since signals were observed at $g = 4$ and not at $g = 6$, the spectrum of Mn(TPP)·I is assigned to an $S = {}^3/_2$ ground state. The absence of signals for an $S = {}^5/_2$ excited state indicates that the antiferromagnetic coupling is sufficiently strong that the population of the $S = {}^5/_2$ level is negligible at 100 K. When two nitroxyl radicals were bound to manganese(II) bis(hexafluoroacetylacetonate) the antiferromagnetic interaction also was strong enough that only the $S = {}^3/_2$ ground state was observed at temperatures below 140 K.[4]

The manganese nuclear hyperfine splitting of the $g = 4$ signal for Mn(TPP)·I was 84 G (Figure 1B). The nuclear hyperfine splitting of the $S = {}^3/_2$ state is 1.2 times the manganese hyperfine splitting in the absence of spin–spin interaction.[11,12] This indicates that the nuclear hyperfine splitting of the noninteracting Mn(III) would be 70 G. The magnitude of this hyperfine splitting is consistent with previous results for manganese(IV) porphyrins (72 G at $g = 4.3$ and 69 G at $g = 2$)[14] and manganese(II) porphyrins (74 G at $g = 5.96$).[15]

As the ratio of the concentration of I to the concentration of Mn(TPP)ClO_4 was increased, the intensity of the signal for Mn(TPP)·I increased and then decreased, which suggested the formation of Mn(TPP)·2I at high nitroxyl concentrations. The bis adduct would have an even number of unpaired electrons and large ZFS and would not be expected to give an EPR spectra.

(5) Landrum, J. T.; Hatano, K.; Scheidt, W. R.; Reed, C. A. *J. Am. Chem. Soc.* **1980**, *102*, 6729.
(6) Sawant, B. M.; Shroyer, A. L. W.; Eaton, G. R.; Eaton, S. S. *Inorg. Chem.* **1982**, *21*, 1093.
(7) More, J. K.; More, K. M.; Eaton, G. R.; Eaton, S. S. *Inorg. Chem.* **1982**, *21*, 2455.
(8) Boymel, P. M.; Braden, G. A.; Eaton, G. R.; Eaton, S. S. *Inorg. Chem.* **1980**, *19*, 735.
(9) Kennedy, B. J.; Murray, K. S. *Inorg. Chem.* **1985**, *24*, 1557.
(10) Behere, D. V.; Mitra, S. *Inorg. Chem.* **1980**, *19*, 992.
(11) Banci, L.; Bencini, A.; Dei, A.; Gatteschi, D. *Inorg. Chem.* **1981**, *20*, 393.
(12) Banci, L.; Bencini, A.; Gatteschi, D. *Inorg. Chem.* **1981**, *20*, 2734.
(13) Bencini, A.; Gatteschi, D. *Transition Met. Chem. (N.Y.)* **1982**, *8*, 1.
(14) Camenzind, M. J.; Hollander, F. J.; Hill, C. L. *Inorg. Chem.* **1983**, *22*, 3776.
(15) Weschler, C. J.; Hoffman, B. M.; Basolo, F. *J. Am. Chem. Soc.* **1975**, *97*, 5278.

The integrated intensity of the $g = 4$ signal was used to monitor the concentration of Mn(TPP)·I. The loss of intensity of the signal for I indicated the total concentration of Mn(TPP)·I and Mn(TPP)·2I. The concentrations of the two complexes were measured as a function of the concentration of I at constant concentrations of $Mn(TPP)ClO_4$. The data are consistent with the equilibria in (1) and (2) with $K_1 = 80 \pm 20\ M^{-1}$ and $K_2 = 120 \pm 40\ M^{-1}$.

$$Mn(TPP) + I \overset{K_1}{\rightleftharpoons} Mn(TPP)\cdot I \quad (1)$$

$$Mn(TPP)\cdot I + I \overset{K_2}{\rightleftharpoons} Mn(TPP)\cdot 2I \quad (2)$$

In a toluene solution containing spin-labeled pyridine, II, and $Mn(TPP)ClO_4$, there was competition between coordination through the nitroxyl oxygen and the pyridine nitrogen. In a solution with 2 mM II and 3 mM $Mn(TPP)ClO_4$, about 30% of the nitroxyl was coordinated to Mn(TPP) via the nitroxyl oxygen. This complex gave a six-line $g = 4$ signal similar to that observed for Mn(TPP)·I (Figure 1B). Thus, the presence of the substituent on the 4-position of the nitroxyl ring had little impact on the lineshape of the spectrum for Mn(TPP)·nitroxyl. When the pyridine nitrogen of II was bound to $Mn(TPP)ClO_4$, the nitroxyl signal was broad and overlapped the spectrum of II that was not coordinated ($g = 2$, not shown in Figure).

The five-membered ring nitroxyls III–VI also coordinated to $Mn(TPP)ClO_4$. The $g = 4$ signals in the EPR spectra of these complexes showed splitting (Figure 1C) that indicated the complex was not axially symmetric. Second-derivative spectra were recorded to improve the resolution of the spectra (Figure 1D). The hyperfine splitting pattern was simulated as two overlapping six-line patterns with slightly different g values and different nuclear hyperfine coupling constants. The values obtained for the spectra of Mn(TPP)·IV that are shown in parts C and D of Figure 1 were $g_1 = 4.014$, $a_1 = 86$ G and $g_2 = 3.990$, $a_2 = 115$ G. Similar parameters were obtained for the complexes with III, V, and VI. The largest variation was in the value of a_2, which ranged from 110 to 115 G. The similarities in the parameters for the five-membered nitroxyl, despite the variation in the nature of the substituents, suggested that the presence of a substituent on the 3-position of the nitroxyl ring was the dominant factor in causing the loss of axial symmetry. A nonaxial spectrum with differences in the manganese nuclear hyperfine splitting for the perpendicular components has also been observed for $Mn(TPP)(O_2)$ ($a_1 = 57$ G, $a_2 = 88$ G).[15]

These results indicate that EPR is a useful tool for examining nitroxyl complexes of metals with even numbers of unpaired electrons.

Acknowledgment. The partial support of this work by NIH Grant 21156 is gratefully acknowledged. Nitroxyls II and IV were prepared by Dr. B. M. Sawant (see ref 6). Nitroxyl V was prepared by Dr. J. K. More (see ref 7).

Registry No. I, 2564-83-2; II, 79991-43-8; III, 3229-73-0; IV, 79991-39-2; V, 81194-35-6; VI, 72444-16-7; $Mn(TPP)ClO_4$, 79408-54-1.

Contribution from the Department of Chemistry,
The Ohio State University, Columbus, Ohio 43210

Reaction Models for Cooperative Catalysis between Metal Ions and Acids or Bases: Hydration and Enolization of Oxalacetate

Suh-Jen Tsai and D. L. Leussing*

Received February 10, 1987

Investigations have been made of cocatalysis between Mg(II), Mn(II), and Zn(II) and the acid and base components of several buffers on the hydration and enolization rates of oxac. The results support preliminary conclusions[2] that complexing metal ion–general-base-cocatalyzed (or OH^--cocatalyzed) enolization processes of $oxac^{2-}$ closely conform to the Marcus function, eq 1, with the same intrinsic barrier, 13.5 kcal mol^{-1}, that is found for enolization in the absence of metal ions. Because of their ability to stabilize the charge developing on the keto oxygen atom as proton abstraction takes place, metal ions bound to $oxac^{2-}$ are even able to activate H_2O as a base catalyst. Stability constants of the intermediate enolate complexes evaluated by fitting the reaction rates to eq 1 are in good agreement with potentiometrically determined values in the case of Mg and Mn. The stability constant obtained for the Zn(II)–enolate by fitting the rate data is consistent with these other values and known trends of complex stabilities with different metal ions. General-acid-catalyzed enolization rates were examined in the context of reaction surfaces proposed in ref 20 and 21 for concerted reactions. The Guthrie surface, modified to conform to eq 1, was found to provide good quantitative agreement between predicted and observed rate constants for reaction paths assumed to involve a concerted reaction of 4-$Hoxac^-$ and the conjugate bases of the nominal general-acid catalysts. Complexed oxac also shows reaction along these same paths, but the models of the reaction surface indicate that the metal ion either partially, or completely, inhibits concerted proton transfer from the 4-CO_2H group. General-base-catalyzed hydration of $oxac^{2-}$ conforms to the modified Guthrie reaction surface. Metal ions increase general-base and OH^--promoted hydration rates owing to the formation of stable complexes with the OH^- addition product. A major solvent-catalyzed hydration pathway is proposed to proceed through a water dimer route. While complexing metal ions also show a prominent solvent-catalyzed pathway, the electrical field surrounding the metal ion may interfere with the water dimer mechanism, but an alternate route involving direct attack of H_2O on the keto carbon is possible.

Recent publications from our laboratory presented evidence that the Marcus function[1] (eq 1) accounts for metal ion rate enhancement observed for the enolization, hydration, and decarboxylation of oxalacetate[2] ($oxac^{2-}$) and the ketonization of enolpyruvate.[3] In eq 1, $\Delta G^{\ddagger}$ represents the actual activation barrier,

$$\Delta G^{\ddagger} = \Delta G^{\ddagger}_0 + \Delta G^{\circ}/2 + (\Delta G^{\circ})^2/16\Delta G^{\ddagger}_0 \quad (1)$$

which is related to the rate constant as given in eq 2; $\Delta G^{\ddagger}_0$ is the

$$\Delta G^{\ddagger} = -1.36 \log k + 17.4\ (25\ ^{\circ}C) \quad (2)$$

intrinsic barrier for the reaction and is the actual barrier when $\Delta G^{\circ} = 0$.

The initial observations indicated that for a given process $\Delta G^{\ddagger}_0$ remains unchanged when the reactants and products are complexed: if K_0 is the known equilibrium constant for the reaction of two uncomplexed ligands, A ⇌ B, and $\Delta G^{\ddagger}_0$ has been evaluated

(1) Marcus, R. A. *J. Phys. Chem.* **1968**, *72*, 891; *J. Am. Chem. Soc.* **1969**, *91*, 7224.
(2) Leussing, D. L.; Emly, M. *J. Am. Chem. Soc.* **1984**, *106*, 443–444.
(3) Miller, B. A.; Leussing, D. L. *J. Am. Chem. Soc.* **1985**, *107*, 7146.

0020-1669/87/1326-2620$01.50/0